

Modification Bentonite Using Fe(III) and Its Application as Adsorbent for Phenol

Muhammad Said *, Widya Twiny Rizki, Widia Purwaningrum, Addy Rachmat, Ferlinahayati, and Poedji Loekitowati Hariani

Department of Chemistry, Faculty of Mathematics and Natural Sciences, Sriwijaya University, Indralaya, Sumatera Selatan, Indonesia

Abstract: Modification of bentonite material using doping Fe(III) was conducted. The purpose of this study is to increase the capacity and effectiveness of bentonite adsorption. The characterization of material was carried out using XRD, XRF, BET and FTIR spectrophotometers. The material produced were used as an adsorbent of phenol in an aqueous medium. The result of characterization material using XRD analysis was showed the difference between unmodified bentonite and modified bentonite, it is indicated from a shift of diffraction peak at 3-10°. The result of XRF analysis was showed the increasing of the iron element on doped bentonite, from 21.3 to 59.11%. The result of BET analysis was showed isotherm adsorption fitted to type IV, which indicates bentonite has a mesoporous type with a size 5-50 nm and natural bentonite has a smaller pore size than activated and doped bentonite. From the FTIR spectrum, there is no chemical interaction between adsorbent and adsorbate. The adsorption rate was fitted to pseudo-first-order. The maximum capacity of phenol adsorption at 60 minutes for controlled was 7.186% and for doped bentonite was 16.4651%. Thermodynamics study explained that the adsorption process occurred spontaneously. It can be concluded that modification bentonite use doping Fe(III) can enhance its ability to adsorbed phenol.

Keywords: adsorption; bentonite; doping; iron (III); phenol.

1. Introduction

One of the organic compounds can be derived from industrial waste is coal, oil and paint, namely phenol. Phenol compounds can be harmful to the environment that can cause unpleasant odors, are toxic and can cause irritation to the skin and even cause death in aquatic organisms¹. Therefore, it is necessary to process phenol. Many ways can be done for the provision of waste containing phenol include using microorganisms², advanced oxidation process³, adsorption processes⁴, membrane filtration⁵ and photocatalysts⁶.

Among the methods, adsorption method is currently used and is considered the most effective method in removing pollutants. The forces that contribute to this adsorption process are the combination of two crucial factors, the adsorbate affinity towards the solvent and the adsorbate affinity towards the adsorbent⁷. Many adsorbents can be used to remove phenol such as bentonite⁸ and activated carbon⁹. One of the adsorbents used for phenol adsorption is bentonite. Based on research¹⁰ were carried out to investigate the possible use of bentonite as an effective adsorbent for removal phenol. The choice of bentonite because it has several advantages such as high porosity level

and easy to find and can be modified in the laboratory¹¹. Bentonite has a cation exchange capacity (CEC) and has hydrophilic properties on its surface so that bentonite can adsorb both organic and inorganic pollutants in the water. However, the ability of bentonite to adsorb organic pollutants, such as phenol, is still less than maximum. For this reason, the adsorption capacity needs to be improved by modifying bentonite¹².

One way to modify bentonite to increase its adsorption capacity is through doping metal on the surface of bentonite. Metals that are usually used in doping are transition metals such as Al¹³ and Fe¹⁴. According to Zu¹⁵, Fe is abundant in nature after Al. The iron used is in the form of Fe (III) can easily be doped on the surface of the bentonite. Therefore, Fe (III) doped bentonite has a high adsorption ability, because Fe can enter the bentonite surface and form complexes with phenolic anion compound¹⁶.

In this study, there were two steps taken — first, modification of bentonite with Fe(III). Second, the phenol adsorption. The products are characterized using XRD, XRF, BET and FTIR spectrophotometer. To measurements of the concentration of phenol, were carried out using a UV-Vis spectrophotometer. The

*Corresponding author: Muhammad Said

Email address: msaidusman@unsri.ac.id

DOI: <http://dx.doi.org/10.13171/mjc9602001021024ms>

Received September 23, 2019

Accepted October 17, 2019

Published January 2, 2020

data will be used to calculate the kinetic and thermodynamic parameters.

2. Experimental

2.1. Materials and Instruments

The materials used in this study were natural bentonite from Lampung, Indonesian, hydrochloric acid (HCl), sodium hydroxide (NaOH), sodium chloric (NaCl), sulfuric acid (H₂SO₄), iron(III) nitrate nanohydrate Fe (NO₃)₃·9H₂O, phenol (C₆H₅OH), sodium hydroxide (NaOH), sodium carbonate (Na₂CO₃), and folin ciocalteu reagent. All the chemicals were analytic grades and supplied by Merck. The distilled water was used in every step of the experiment.

2.2. Characterization of material

The functional groups were determined by Fourier Transform Infrared (FTIR Thermo Scientific Nicolet iS10). The identification of phases or rock-forming compounds can be done using the X-Ray Diffraction (XRD Bruker D8 Advance method) while the analysis of metal and non-metal elements as a whole can be done with the X-Ray Fluorescence (XRF Malvern PANanalytical). The surface area of the material was mapped by the BET method using N₂ adsorption-desorption (Nova 4200e).

2.3. Preparation of Fe (III) Doping Solution

Preparation of Fe (III) doping solution was carried out by adding Fe (NO₃)₃·9H₂O 0.5M as much as 40 mL mixed into 500 mL beaker and then pouring 0.5 M NaOH solution as much as 240 mL. Then the mixture was sterilized for 24 hours then left at room temperature for 2 days.

2.4. Process of Fe(III) Doped onto Bentonite

Fe(III) doped bentonite was synthesized by adding 12 g of activated bentonite into 120 mL of distilled water while stirring for 24 hours. The Fe(III) dopant was added and stirred for 24 hours at room temperature, centrifuged with 4000 rpm for 10 min, and then the precipitate was dried in an oven at 100°C for 48 hours. Fe(III) doped bentonite obtained was characterized by XRD, XRF, BET and FT-IR spectrophotometer.

2.5. Measurement of Point Zero Charge of activated Bentonite and Fe (III) Doped Bentonite

Measuring the zero charge point was done by preparing 50 mL of NaCl solution 0.1 M and set the initial pH of 2, 3, 4, 5, 6, 7, 8, 9 and 9. The pH set was made by adding NaOH 0.01 M, and HCl 0.01 M. Then added 0.05 g of activated bentonite and 0.05 g of Fe (III) doped bentonite into the pH-adjusted. Then the mixture was shaken for 24 hours, and then measured by a pH meter so that the final pH was obtained and graphed.

2.6. Effect of Adsorption Time and Kinetic Parameters

The effect of adsorption kinetics by activated and Fe(III) doped bentonite was done by adding as much

as 0.03 g of activated bentonite into 30 mL phenol with a concentration of 100 mg/L. The mixture was stirred with a shaker at a predetermined time interval (20, 30, 40, 50, 60 and 70 min). After the adsorption process, the phenol was separated. The filtrate was taken 5 mL, added with 0.5 mL folin ciocalteu and 1 mL Na₂CO₃ 20% reagents. The solution is homogenized and left for 30 minutes. After that, each absorbance was measured using a UV-Vis spectrophotometer. The same procedure was done with Fe(III) doped bentonite. The amount of adsorbed phenol (mg/L) was calculated using the standard solution calibration curve equation. The adsorption rate is determined using adsorption kinetic data following pseudo-first-order and pseudo-second-order equations:

$$\log(Q_e - Q_t) = \log Q_e - \left(\frac{k_1}{2.303}\right) t \quad (1)$$

$$\frac{t}{Q_t} = \frac{1}{k_2 Q_e^2} + \frac{1}{Q_e} t \quad (2)$$

Where Q_e is the amount of adsorbate adsorbed at equilibrium (mg/gr), Q_t is the amount of adsorbate adsorbed at time t (mg/gr), k_1 is 1st order adsorption rate (min⁻¹), k_2 is 2nd order adsorption rate (g.mg⁻¹min⁻¹), and t is time (min).

Adsorption isotherms are calculated based on the Langmuir and Freundlich equations as follows:

$$\frac{C_e}{Q_e} = \frac{C_e}{Q_m} + \frac{1}{Q_m K_L} \quad (3)$$

$$\log Q_e = \log K_F + 1/n \log C_e \quad (4)$$

Where C_e is the concentration of phenol solution at equilibrium (mg/L), Q_m is the maximum adsorption capacity (mg/g), K_L is the Langmuir constants, K_F is the Freundlich constants, Q_e is the adsorption capacity at equilibrium (mg/g).

2.7. Effect of Concentration, Temperature, Isotherm and Thermodynamic Parameters

The isotherm and thermodynamic parameters of phenol adsorption were carried out through a series of experiments by varying phenol concentration and adsorption temperature. A total of 0.05 g of adsorbent of activated bentonite were mixed with 50 mL of phenol with the concentration of 25, 50, 75, 100 and 150 mg/L. The adsorbent mixed with phenol was stirred using a horizontal shaker for 80 minutes at various temperatures (30, 40, 50, 60 and 70 °C). The mixture was separated, then the phenol solution diluted 10 times and measured the absorbance value using a UV-Vis spectrophotometer to determine the concentration of the remaining phenol. The same procedure is performed for Fe(III) doped bentonite. The thermodynamic parameters in the form of enthalpy, entropy, and Gibbs free were calculated using the formula:

$$\frac{Qe}{Ce} = \frac{\Delta S}{R} - \frac{\Delta H}{RT} \quad (5)$$

$$\Delta G = \Delta H - T\Delta S \quad (6)$$

Where E is the adsorption energy (kJ/mole), R is Constants, T is Temperature, Qe/Ce is Coefficient of distribution of adsorbate, ΔH is the Enthalpy (kJ/mole), ΔS is Entropy (kJ/Kmole).

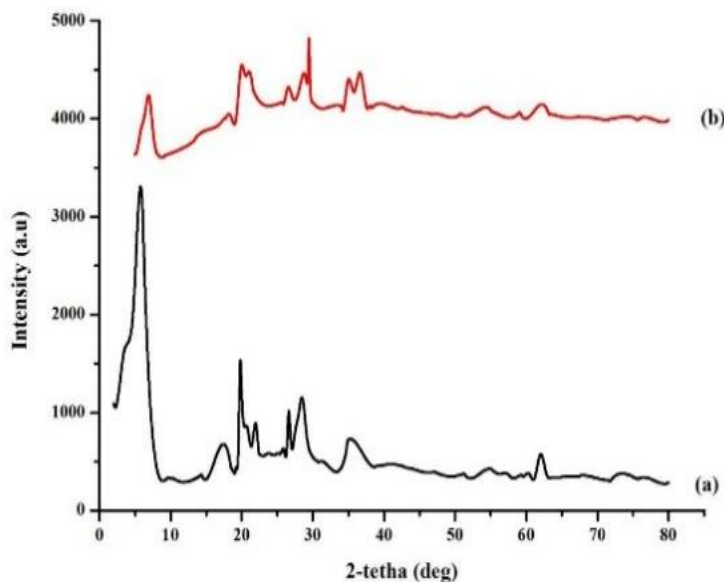


Figure 1. XRD spectrum: (a) Activated bentonite, (b) Fe(III) doped bentonite

According to Bertella and Pergher¹⁸, bentonite will experience changes in XRD diffraction patterns when doped by atoms, molecules and compounds. From [Figure 1](#) it shows the difference in diffraction patterns of activated and Fe(III) doped bentonite. This difference can be seen from the diffractogram that appears or disappears at a certain angle. For example, in [Figure 1a](#) around an angle of 2θ , i.e. 28° the peak formed is not too sharp, while in [Figure 1b](#) around the angle 2θ , i.e. 28° there appears a sharp peak rise. This shows that at this angle, other elements appear in the bentonite content, and it can be ascertained that the angle appears due to the addition of Fe to the bentonite. The next difference can be seen in the characteristics of the diffraction peak. In [Figure 1a](#), activated bentonites exhibit characteristics of the montmorillonite (2θ) diffraction peak around 5.671° ; 17.53° ; 19.738° ; 35.03° and 61.94° , while in [Figure 1b](#), Fe(III) doped bentonite shows a diffraction peak at the peak of montmorillonite at an angle of 2θ which is around 7.04° ; 20.041° ; 28.68° ; 29.438° ; 36.59° and 62.04° . From the results of XRD characterization, it can be concluded that activated bentonite has a characteristic angle at 5.671° and after doping using Fe(III) there is an angle shift to 7.04° . This means that bentonite has a shift in angle from a smaller angle to a larger angle. These angular changes indicate the presence of other cations in the form of Fe(III) found in the inter-field of bentonite¹⁹.

3. Results and Discussion

3.1. Characterization of Controlled Bentonite and Fe (III) Doped Bentonite Using XRD

The results of the characterization of activated and Fe(III) doped bentonite using XRD were aimed at seeing changes at the peak of diffraction (2θ). The successful of doping of Fe(III) onto bentonite surface can be seen from the shift of the diffraction peak (2θ) at an angle of $3-10^\circ$ ¹⁷ as shown in [Figure 1](#).

3.2. Characterization of Activated and Fe (III) doped bentonite Using XRF

Characterization using XRF aims to see the composition of metals found inactivated and Fe(III) doped bentonite. In [Figure 2](#) shows that activated bentonite contains a percentage of Al, Si, K, Ca, Fe, Cu, and Cr metal composition were 15.05; 56.6; 1.06; 4.27; 21.3; 1.084 and 0.636%, respectively. Fe (III) doped bentonite contains a percentage of Al, Si, K, Ca, Fe, Cu, and Cr metal composition were 7.6; 29.3; 0.34; 3.34; 59.11; 0.17 and 0.14%, respectively. The composition of Al, Si, K, Ca, Cu, and Cr metals decreased while the Fe increased. It proves the cation exchange between Fe metal and metals in bentonite composition. The result of the chemical composition in bentonite similar to those of previous workers²⁰. The complete composition of metals before and after the doping process can be seen in [Table 1](#).

Table 1. The composition of Fe metal before and after the doping process.

Sample	Fe (%)
Controlled bentonite	21.3
Doped bentonite	59.11

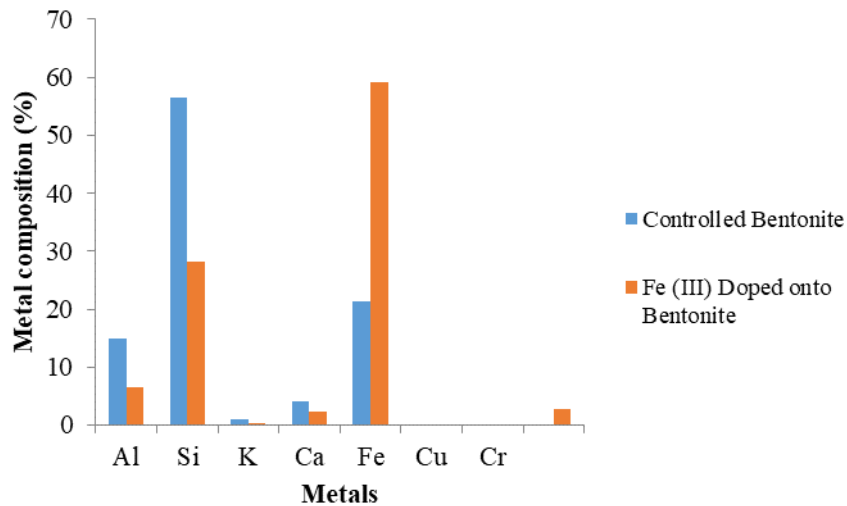


Figure 2. Metal composition for controlled bentonite and Fe(III) doped onto bentonite

3.3. Characterization of Natural Bentonite, Activated Bentonite (Controlled) and Fe(III) Doped onto Bentonite Using BET

Natural bentonite activated bentonite and Fe(III) doped bentonite were characterized by nitrogen adsorption-desorption, so data on the surface area,

pore volume and pore size were obtained through a calculation using BET which will be directly obtained from the measurement data. The adsorption-desorption nitrogen isotherm for natural bentonite, activated, and Fe (III) doped bentonite can be seen in [Figure 3](#).

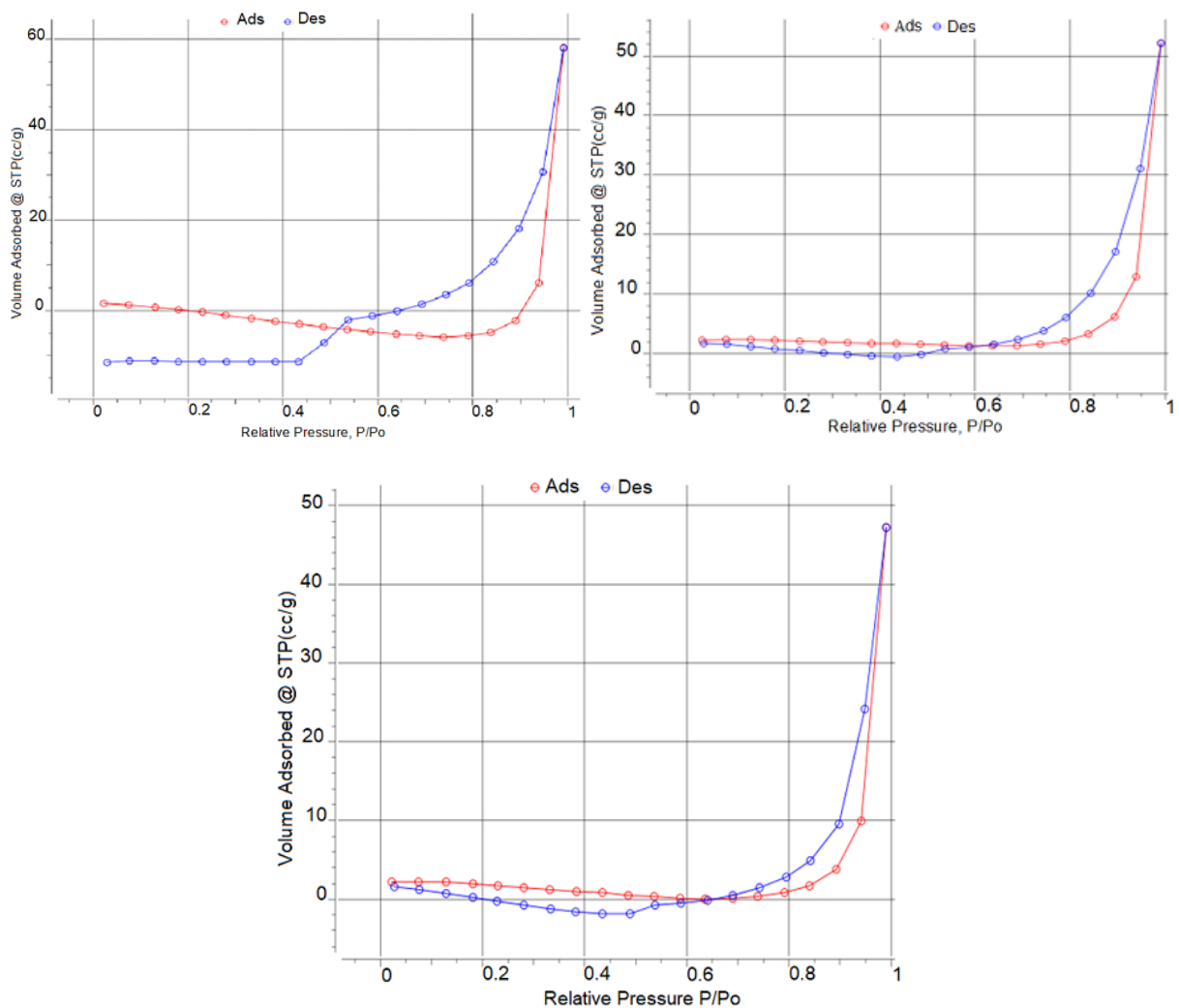


Figure 3. Nitrogen adsorption and desorption profile: (a) natural bentonite, (b) activated bentonite and (c) Fe(III) doped onto bentonite

The image shows that the isotherm match in type IV. This type usually occurs on porous adsorbents with a pore size of 1.5 - 100 nm, which includes pore size in the form of mesoporous to macropore. While at high pressure shows an increase in adsorption of adsorbate that makes pores significant ²¹. The red line on the isotherm graph shows the process of nitrogen gas adsorption in natural bentonite, activated bentonite

and Fe(III) doped bentonite while the blue line shows the desorption process. We know, that the existence of impurities in samples can break the material due to activation and doping by Fe(III) so that the material becomes low in volume adsorption by nitrogen gas. BET results data for natural bentonite, activated, and Fe (III) doped bentonite are presented in Table 2.

Table 2. BET Results Data.

	Surface Area (m ² /g)	Pore Diameter BJH (nm)	Pore Volume BJH (cm ³ /g)
Natural	6.464	13.211	0.105
Controlled	6.060	13.263	0.083
Doped	5.166	13.559	0.077

Based on the data in Table 2, it can be concluded that bentonite doped with Fe(III) has a smaller surface area compared to natural bentonite and activated bentonite. This is caused by the doping process using Fe(III), which is large enough to increase pore size because it can reduce the density of bentonite. The addition of Fe(III) to bentonite causes the concentration of Fe in bentonite to increase, causing the pore diameter to increase and the surface area to decrease ²².

3.4. Identification of Activated Bentonite, Fe (III) Doped Bentonite and Phenol Adsorption Results by Using FT-IR Spectrophotometer

The activated and Fe(III) doped bentonite, both for before and after adsorbing phenol were characterized using FT-IR spectrophotometer. Characterization aims to identify functional groups in activated bentonite, Fe(III) doped bentonite and bentonite after the adsorption process. The FT-IR spectrum is presented in Figure 4.

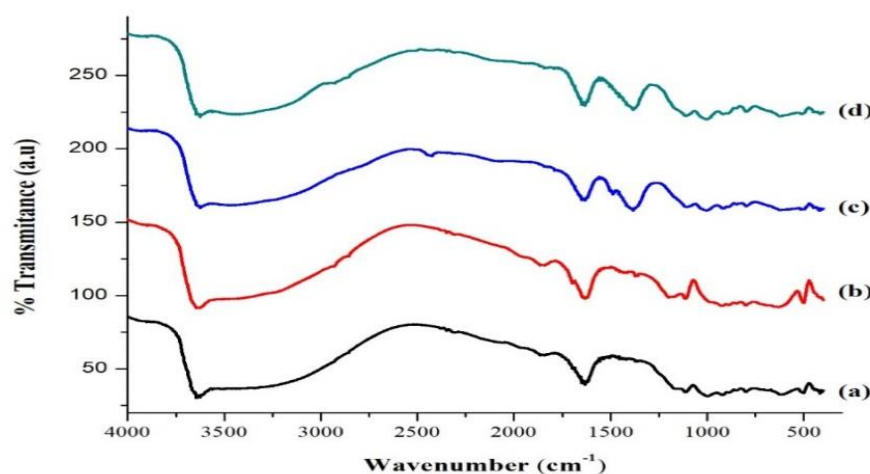


Figure 4. FT-IR spectrum: (a) activated bentonite, (b) activated bentonite after adsorbing phenol, (c) bentonite doped with Fe(III), and (d) Fe(III) doped bentonite after adsorbing phenol

In Figure 4, it can be seen that there is a change in IR spectrum that is not too significant. It is seen that there is a typical absorption band on bentonite at wave number 3600 cm⁻¹ and 1600 cm⁻¹ that shows Al-O-(OH)-Al and Al-bending strain vibration. O-(OH)-Al as an octahedral layer in bentonite. Si-O-Fe that appears at a wavenumber of 500 cm⁻¹ ²³.

Based on FTIR data in Figures 4a and 4b above at wave number 1100 cm⁻¹ that is known as the presence of C-O phenol, the peak narrowing occurs. At 1400 cm⁻¹ wavenumber peak was identified as the presence of C-C phenol. At 1800 cm⁻¹ wave number there is also widening identified as Fe-O. In Figure 4a and 4c there are differences in the shape of the FTIR spectrum, namely the emergence of a peak at wave

number 1400. The appearance of the peaks in Figure 4c is identified as the presence of C-C phenol. There are also differences in Figures 4a and 4d, namely the appearance of two peaks at wavenumber 1400 cm⁻¹ and those identified as the presence of C-C phenol. In Figures 4b and 4d, FTIR spectrum differences occur. It can be seen in Figure 4d; two peaks appear at wave number 1400 cm⁻¹ and 1600 cm⁻¹. In Figures 4c and 4d there is also a narrowing of the peak at the wave

number 1100 cm⁻¹ which is identified as the presence of C-O phenol. At 1400 cm⁻¹ wavenumber peak was identified as the presence of C-C phenol.

Doped bentonite, which has absorbed phenol was characterized using FT-IR spectrophotometer, which is presented in Figure 4. It can be seen from the FT-IR spectrophotometer data that there was no change and significant shift of absorption band from activated bentonite, activated bentonite after absorbing phenol, doped bentonite Fe(III) and bentonite doped after absorbing phenol. In the spectrum, it is said that there is a bond between bentonite and Fe, while the phenol adsorption process is not clearly observed.

3.5. Point Zero Charge (PZC) Analysis

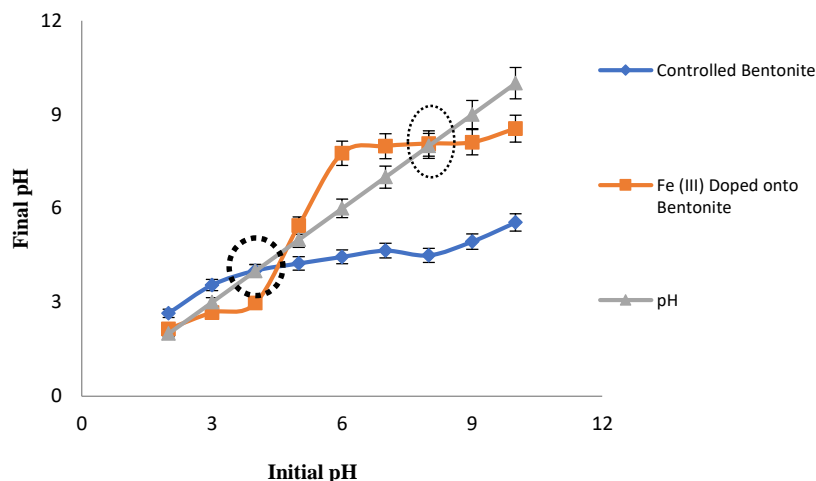


Figure 5. pHpzc analysis

Based on Figure 5, it can be seen that there is no change in the initial and final pH values at pH 4 and 8. This shows that the pHpzc value is at pH 4 for activated bentonite and pH 8 for Fe(III) doped bentonite. The difference in the pHpzc value is due to differences in the acidity of activated and Fe(III) doped bentonite ²⁴.

3.6. Phenol Adsorption Using Activated Bentonite and Fe (III) Doped Bentonite

3.6.1. Effect of Adsorption Time and Kinetic Parameter Determination

The effect of phenol adsorption time by activated and Fe(III) doped bentonite was aimed to find the optimum time in the phenol adsorption process.

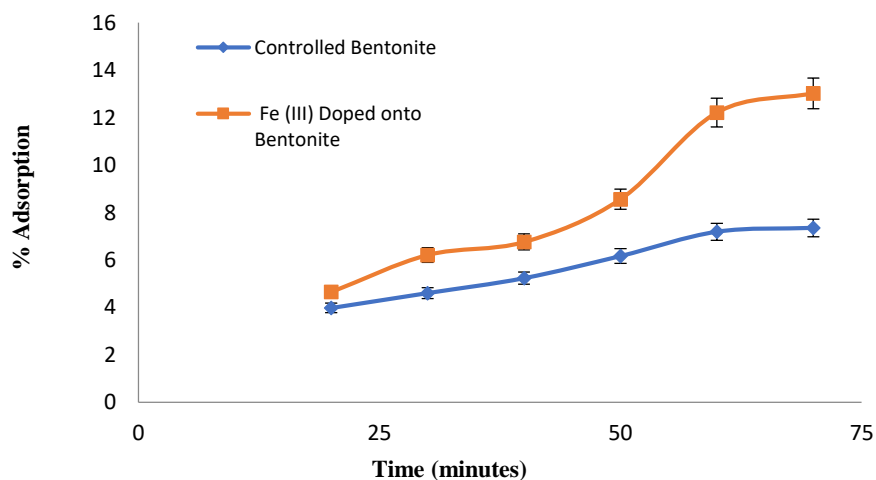


Figure 6. Effect of contact time of adsorption of activated bentonite and Fe(III) doped bentonite on phenol

The effect of time is an essential factor in the adsorption process to see collision interactions between adsorbents and adsorbate. The adsorption

time was varied, namely 20, 30, 40, 50, 60, 70. The residual concentration of phenol was calculated using a UV-Vis spectrophotometer with a wavelength of

650.5 nm. The following curve of the effect of time on the amount of phenol is presented in Figure 6.

In Figure 6 it can be seen that Fe (III) doped bentonite absorbs more adsorbate than activated bentonites at the same time. The percentage of adsorption for activated bentonite increases with increasing adsorption time; this is due to the collision between the adsorbent and the adsorbate. Percentage of adsorption for Fe (III) doped bentonite increased and decreased because the phenol, which was adsorbed at that time, was not yet stable. The optimum time for adsorption of bentonite activated against phenol is 60 minutes. Activated and Fe (III) doped bentonite at 60 minutes reached equilibrium, percent adsorption was 7.18% and 16.46%. This is because after reaching the optimum time, the surface side of the adsorbent will be fulfilled with phenol so that it cannot absorb the adsorbate²⁵. It should be noted that the more the initial phenol concentration, the more would be the

adsorption capacity of adsorbent, but the adsorption efficiency of adsorbent was inversely related to the initial phenol concentration, and the removal efficiencies decreased as the concentration increase at a fixed adsorbent dosage²⁶. The result shows that an increase in initial phenol concentration would lead to a decrease in the rate of constant values, which are in agreement with the study before²⁷.

From the data of the effect of adsorption time, data were obtained to calculate the adsorption rate using the first order pseudo equation and the pseudo-second-order. The adsorption rate is the adsorption power of activated and Fe(III) doped bentonite which can adsorb phenol at specific concentrations and times. The kinetic model calculation data is presented in Table 3.

Table 3. The kinetic model constants of phenol adsorption on the effect of time.

Adsorbent	Q_{exp} (mg/g)	Pseudo-first-order			Pseudo-second-order		
		Q_e (mg/g)	k_1	R^2	Q_e (mg/g)	k_2	R^2
Controlled Bentonite	7,18	10,51	0,03	0,94	12,3	0,001	0,94
Doped Bentonite	16,46	14,44	0,03	0,4	18,72	0,0004	0,16

From the data obtained in Table 3 shows the adsorption of phenol on activated bentonite using the Pseudo-first-order and Pseudo-second-order kinetic adsorption model because the correlation coefficient (R^2) of Pseudo-first-order is the same as the Pseudo-second-order. Fe (III) doped Bentonite does not occur in Pseudo-first-order or Pseudo-second-order equations, so it does not follow the two equations²⁸.

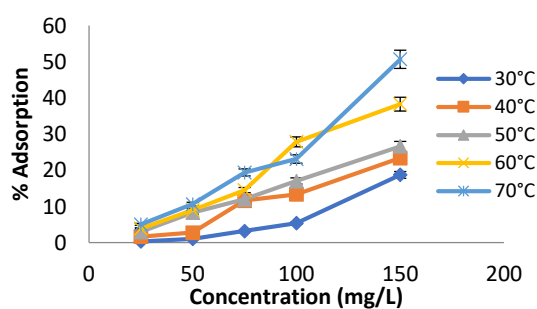


Figure 7. Effect of phenol concentration and temperature on activated bentonite

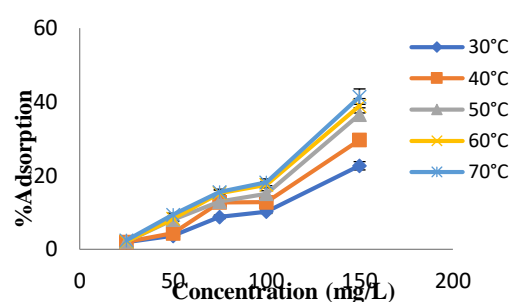


Figure 8. Effect of phenol concentration and temperature on Fe (III) doped bentonite

In Figure 7 and Figure 8, it can be seen that the higher the concentration and temperature the per cent adsorption will increase. The adsorption process with the effect of phenol concentration at various temperatures was calculated based on the Langmuir equation and the Freundlich equation. The Langmuir

Isotherm model can explain the adsorption process on the adsorbent that occurs on the surface of the adsorbent and adsorption occurs monolayer, whereas the Freundlich adsorption isotherm model can be used to predict the adsorption capacity of the adsorbent. The data are presented in Table 4.

Table 4. Data on adsorption isotherm using the Langmuir model and Freundlich

Temp. (°C)	Model isotherm Langmuir			Model isotherm Freundlich		
	Parameter	Controlled Bentonite	Fe (III) doped onto bentonite	Parameter	Controlled Bentonite	Fe (III) doped onto bentonite
30	K_L (L/mg)	0.0076	4.5785	K_F	0.0001	0.0204
	Q_m (mg/g)	1.7082	16.0513	n	0.4281	0.7059
	R^2	0.8870	0.7559	R^2	0.9742	0.9626
50	K_L (L/mg)	0.0031	0.0063	K_F	0.0681	0.0148
	Q_m (mg/g)	46.5116	15.8478	n	0.8001	0.6152
	R^2	0.5585	0.6384	R^2	0.9889	0.9616
70	K_L (L/mg)	0.0049	0.0068	K_F	0.0819	0.0158
	Q_m (mg/g)	45.4545	17.1526	n	0.7395	0.6013
	R^2	0.7712	0.6219	R^2	0.9623	0.9627

The adsorption isotherm using the Freundlich model has better adsorption than the Langmuir model. The coefficient of relations (R^2) of the Freundlich model has a higher value than the Langmuir model. This shows that in phenol adsorption using activated and Fe (III) doped bentonite is more suitable using the Freundlich isotherm model. Freundlich isotherm is an empirical equation based on the assumption of multilayer formation of adsorbate and that adsorption take place on heterogeneous surface ²⁹.

The thermodynamic parameters of adsorption include enthalpy (ΔH), entropy (ΔS), Gibbs free energy (ΔG). The values of enthalpy (ΔH) and entropy (ΔS) can be calculated as slope and intercept values of $1/T$ against $\ln Q_e/C_e$. The value of the change in Gibbs free energy (ΔG) is calculated from the enthalpy value (ΔH) and entropy (ΔS). Data on the effect of temperature on phenol adsorption on activated and Fe (III) doped bentonite can be seen in Table 5.

Tables 5 show the value of adsorption capacity (Q_e) increases with increasing temperature for the

adsorbent of activated and Fe (III) doped bentonite. It can be seen that the adsorption capacity of Fe (III) doped bentonite is higher than that activated bentonite. This is because the doping process causes the surface pore to be slightly larger so that the material capacity to adsorb becomes larger. The adsorption capacity also increases with increasing concentration ³⁰.

From Tables 5, which present enthalpy data (ΔH) and (ΔS) tend to decrease with the concentration of phenol. The value (ΔH) marked positive indicates an endothermic reaction. Gibbs free energy (ΔG) shows that in natural bentonite adsorbent (activated) there is a tendency to decrease Gibbs free energy (ΔG) with increasing temperature. The same thing happened to the adsorbent of Fe (III) doped bentonite with increasing temperature. Gibbs free energy also tends to decrease. ΔG has a negative sign indicating the reaction is spontaneous.

Table 5. Data of Entropy (ΔS), Enthalpy (ΔH), free energy Gibbs (ΔG), and Adsorption capacity (Q_e).

Conc. (mg/L)	Temp. (K)	Controlled bentonite				Doped bentonite				
		Q_e (mg/g)	ΔS (kJ/mole)	ΔH (kJ/mole)	ΔG (kJ/mole)	Q_e (mg/g)	ΔS (kJ/mole)	ΔH (kJ/mole)	ΔG (kJ/mole)	
50	303	0.349	0.2847	-97.616	-11.350	3.695	0.074	-39.040	-6.467	
	313	2.791			-8.503				4.364	-5.722
	323	8.326			-5.656				8.060	-4.977
	333	9.047			-2.809				8.337	-4.232
100	303	5.419	0.1442	-50.601	-6.908	10.230	0.039	-29.263	-5.452	
	313	13.349			-5.466				12.817	-5.060
	323	17.047			-4.024				15.127	-4.668

	333	27.860			-2.582	17.528			-4.276
150	303	18.767	0.060	-23.196	-5.016	22.702	0.050	-19.384	-4.234
	313	23.407			-4.416	29.676			-3.734
	323	26.651			-3.816	36.605			-3.234
	333	38.302			-3.216	38.937			-2.734

4. Conclusion

Based on the results of the characterization of activated and Fe (III) doped bentonite using XRD, XRF, BET and FTIR spectrophotometer Fe (III) doping process on bentonite can increase adsorption capacity and effectiveness. Phenol adsorbed by activated bentonite reached 7.186% less than phenol adsorbed by Fe (III) doped bentonite that reached 16.465%. Based on the kinetics calculation on activated bentonite, the adsorption kinetics used to meet Pseudo-first-order and Pseudo-second-order equations.

Meanwhile, the isotherm model used is a Freundlich isotherm model, which means that the adsorption process takes place physically. Based on thermodynamic calculations. Enthalpy and entropy values inactivated and Fe (III) doped bentonite tend to decrease with increasing phenol concentration. The Gibbs free energy value with a negative sign indicates the reaction is spontaneous.

5. Acknowledgements

The author would like to thank Universitas Sriwijaya for funding through scheme Hibah Penelitian Unggulan Kompetitif 2019 grants 0149.162/UN9/SB3.LP2M.PT/2019.

References

- 1- S. Slamet, A. Putera, S. Bismo, Performance Test with TiO₂ Modified Activated Carbon on Pilot Scale Phenol Removal, *The Journal for Technology and Science*, **2008**, 19(4), 117-122.
- 2- N.A. Boroujeni, M. Hassanshahian, S.M.R. Khoshrou. Isolation and characterization of phenol degrading bacteria from the Persian Gulf, *International Journal of Advanced Biological and Biomedical Research*, **2014**, 2(2), 408-416.
- 3- A. Rubalcaba, M.E. Suarez-Ojeda, F. Stuber, A. Fortuny, C. Bengoa, I. Metcalfe, J. Font, J. Carrera and A. Fabrega. Phenol wastewater remediation: advanced oxidation processes coupled to biological treatment, *Water Science & Technology*, **2007**, 55(12), 221-227.
- 4- P.L. Hariani, Fatma, F. Riyanti, H. Ratnasari, Adsorption of Phenol Pollutants from Aqueous Solution Using Ca-Bentonite/Chitosan Composite. *Journal Manusia dan Lingkungan*, **2015**, 22(2), 233-239.
- 5- M.Said, A. Ahmad and A.W. Mohammad, Removal of phenol during ultrafiltration of Palm oil mill effluent (POME): Effect of pH, ionic strength, pressure and temperature, *Der Pharma Chemica*, **2013**, 5(3), 190-196.
- 6- M.M. Ba-Abbad, M.S. Takriff, M. Said, A. Benamor, M.S. Nasser, A.W. Mohammad, Photocatalytic Degradation of Pentachlorophenol Using ZnO Nanoparticle, *International Journal of Environmental Research*, **2017**, 11(4), 461-473.
- 7- M.M. Lynam, J.E. Kilduff, W.J. Weber. Adsorption of p-Nitrophenol from Dilute Aqueous Solution. *Journal Chemical Education*, **2005**. 72(1), 80-85.
- 8- Y.H. Shen. Removal of Phenol from Water by Adsorption –Flocculation Using Organobentonite. *Water Research*. **2002**. 36, 1107- 1114.
- 9- V. Srihari and A. Das. Adsorption of Phenol from Aqueous Media by an Agro Waste Based Activated Carbon. *Applied Ecology and Environmental Research*, **2009**. 7(1), 13-23.
- 10- E. Aznar, M.S. Yusi, Y. Bow. Purification of Crude Glycerol from Biodiesel By-product by Adsorption using Bentonite. *International Journal of Fundamental and Applied Chemistry*, **2018**, 3(3), 83-88.
- 11- S. Slamet, A. Putera, S. Bismo, Performance Test with TiO₂ Modified Activated Carbon on Pilot Scale Phenol Removal, *The Journal for Technology and Science*, **2008**, 19(4), 117-122.
- 12- F. Bergaya and M.S. Vayer, CEC of Clays: Measurement by adsorption of a copper ethylenediamine complex, *Applied Clay Science* 12, Perancis, **2006**, University of Grenoble.
- 13- M. Harmankaya and G. Gunduz, Catalytic oxidation of phenol in aqueous solution, *J. Eng. Environment Science*, **2015**, 22(1), 9-15.
- 14- M.Said, H.P. Utami, F. Hayati. Insertion of bentonite with Organometallic [Fe₃O(OOC₆H₅)₆(H₂O)₃(NO₃)_nH₂O] as Adsorbent of Congo Red, *IOP Conference Series: Materials Science and Engineering*, **2018**, 299(1), 1-9.
- 15- Z.X. Feng and X.X. Hua. The Mechanism of Fe (III) Catalyzed of Phenol, *J. Zhejiang Univ. Sci*, **2004**, 5(12), 1543-1547.
- 16- S. Y. Rahni, B. Rezaei, N. Mirghaffari, Bentonite surface modification and characterization for high selective phosphate adsorption from aqueous media and its application for wastewater treatments, *Journal of Water Reuse and Desalination*, **2016**, 7 (2), 175-186.
- 17- H. Z. Boudiaf, M. Boutahala, S. Sahnoun, C. Tiar, F. Gomri, Adsorption Characteristics, Isotherm, Kinetics, and Diffusion of Modified Natural Bentonite for Removing The 2,4,5-Thrchlorophenol,

- Applied Clay Science, **2014**, 81-87.
- 18-F. Bertella and S. B. C. Pergher, Doping of Bentonite Clay with Al and Co, Microporous and Mesoporous Materials, **2014**, 201, 116-123.
- 19-H. Z. Boudiaf, M. Boutahala, S. Sahnoun, C. Tiar, F. Gomri, Adsorption Characteristics, Isotherm, Kinetics, and Diffusion of Modified Natural Bentonite for Removing The 2,4,5-Thrichlorophenol, Applied Clay Science, **2014**, 81-87.
- 20-A. Tabak, B. Afsin, B. Caglar, E. Koksak. Characterization and Pillaring of a Turkish Bentonite. Journal of Colloid and Interface Science. **313**(1), 5-11.
- 21-H.I. Lee, H.J. Park, Y. Park, J.Y. Hur, J. Jeon, J.M. Kim, Synthesis of highly stable mesoporous aluminosilicates from commercially available zeolites and their application to the pyrolysis of woody biomass, Journal of Interface Science, **2008**, 132, 68-7.
- 22-N.A. Pradisty, R. Sihombing, R.F. Howe, Y.K. Krisnandi, Fe(III) Oxide-modified Indonesian Bentonite for Photodegradation of Phenol in Water, Makara Journal of Science, **2017**, 21(1), 25-33.
- 23-L. Perelomov, B. Sarkar, M. Rahman, A. Garyacheva, R. Naidu. Uptake of Lead by Na-Exchanged and Al-Pillared Bentonite in The Presence of Organic Acids with Different Functional Groups. Applied Clay Science, **2016**, 119, 417-423.
- 24-V. Masindi, M.W. Gitari, H. Tutu, Adsorption of Oxyanions from Coal Fly Ash Leachates Using Bentonite. South Africa: LAP Lambert Academic Publishing **2016**.
- 25-H.B. Senturk, D. Ozdes, A. Gundogdu, C. Duran, M. Soylak, Removal of Phenol from Aqueous Solutions by Adsorption onto Organomodified Tirebolu Bentonite: Equilibrium, kinetic and Thermodynamic Study. Journal of Hazardous Materials, **2009**, 172(1), 353-362.
- 26-L.J. Kenned, J.J Vijaya, K. Kayalvizhi, G. Sekaran, Adsorption of Phenol from Aqueous Solution Using Mesoporous Carbon Prepared by Two-stage Process. Chem Engin J., **2007**, 132(3), 87-279.
- 27-B. Benguella and H. Benaissa. Cadmium Removal from Aqueous Solution by Chitin: Kinetic and Equilibrium Studies. Journal Water Res. **2002**. 36(10), 2463-74.
- 28-J.A. Alexander, M.A.A. Zaini, A. Surajudeen, E.U. Aliyu, A.U. Omeiza, Surface Modification of Low-Cost Bentonite Adsorbent. International Journal Particulate Science and Technology, **2018**, 37(5), 534-545.
- 29-A. Behnamfard and M.M. Salarirad, Equilibrium and Kinetic Studies on Free Cyanide Adsorption from Aqueous Solution by Activated Carbon. Journal Hazard Mater. **2009**. 170(1), 33-127.
- 30- S. Lyubchik, A. Lyubchik, O. Lygina, S. Lyubchik, I. Fonseca. Comparison of the Thermodynamic Parameters Estimation for the Adsorption Process of the Metals from Liquid Phase on Activated Carbons, Thermodynamics - Interaction Studies - Solids, Liquids and Gases, **2011**, Intech Open, London, United Kingdom.